frontiers in Earth Science

ORIGINAL RESEARCH
published: 25 February 2022
doi: 10.3389/feart.2022.844026

Correlation Between brGDGTs Distribution and Elevation From the Eastern Qilian Shan

Hansheng Wang†, Peng Gao†, Rui Yang†, Junsheng Nie, Bo Cao, Aifeng Zhou*, Baotian Pan*, Lin Chen and Tingjiang Peng*

Key Laboratory of Western China's Environmental Systems (Ministry of Education) , College of Earth and Environmental Sciences, Lanzhou University, Lanzhou, China

OPEN ACCESS

Edited by:
Yongli Wang, Institute of Geology and Geophysics (CAS), China

Reviewed by:
Weiguo Liu, Institute of Earth Environment (CAS), China
Zhifu Wei, Institute of Geology and Geophysics (CAS), China

***Correspondence:**
Junsheng Nie
jnie@lzu.edu.cn
Aifeng Zhou
zhouaf@lzu.edu.cn
Baotian Pan
panbt@lzu.edu.cn

†These authors have contributed equally to this work

Specialty section:
This article was submitted to Quaternary Science, Geomorphology and Paleoenvironment, a section of the journal Frontiers in Earth Science

Received: *27 December 2021*
Accepted: *25 January 2022*
Published: *25 February 2022*

Citation:
Wang H, Gao P, Yang R, Nie J, Cao B, Zhou A, Pan B, Chen L and Peng T (2022) Correlation Between brGDGTs Distribution and Elevation From the Eastern Qilian Shan. Front. Earth Sci. 10:844026. doi: 10.3389/feart.2022.844026

A clear understanding of the uplift history of the Tibetan Plateau is the key for correctly understanding its uplift mechanisms and impacts on the Asian environment. However, consensus has not been reached regarding the uplift history of the Tibetan Plateau, especially because of lack of well-calibrated paleoaltimetry proxies and lack of knowledge of how to correctly apply them to the past. Branched glycerol dialkyl glycerol tetraethers (brGDGTs) are a promising paleoaltimetry proxy because these large molecules tend to get preserved in sediments, and this proxy has a clear relationship with mean annual air temperature (MAAT), circumventing convoluted impact of precipitation or isotope variations on isotope-based paleoaltimetry proxies. As a result, many calibrations have been carried out linking brGDGTs with paleoelevation. Qilian Shan of the northeastern Tibetan Plateau is a key place testing previous models regarding the uplift model of the Tibetan Plateau. However, no modern calibration equation linking brGDGTs with MAAT is available. Here, we presented the first calibration equation between brGDGTs and MAAT from the eastern Qilian Shan with an elevation ranging from 2,055 to 3,300 m [MAAT = −15.50 + 49.55 × MBT'_{5ME} (R^2 = 0.89, $p < 0.001$, RMSE = 1.07°C)]. We further established the calibration between MBT'_{5ME}-derived MAAT and elevation. This dataset lays the foundation to understand the uplift history and environmental variations of the northeastern Tibetan Plateau area.

Keywords: Qilian Shan, brGDGTs, MBT'_{5ME}, elevation, paleo-altimeter, calibration equation

INTRODUCTION

The Tibetan Plateau is the largest orogenic belt, known as "the Roof of the World" (Fielding, 1996; Yin and Harrison, 2000; Royden et al., 2008). The uplift of the Tibetan Plateau over the Cenozoic is considered a key forcing for regional and global climate (An et al., 2001; Molnar et al., 2010), but its uplift history is hotly debated (Harrison et al., 1992; Raymo and Ruddiman, 1992; Molnar et al., 1993; Liu and Yin, 2002; Chung et al., 2005; Lu et al., 2005; Liu et al., 2016). Different models have been proposed regarding the uplift of the Tibetan Plateau, and the northeastern Tibetan Plateau is a key location to test these models because they predicted different uplift timing of this part of the plateau (Harrison et al., 1992; Kristen Clark and Handy Royden, 2000; Tapponnier et al., 2001). For example, stepwise uplift models emphasizing large-scale strike-slipping faulting in establishing the plateau predicted Pliocene–Pleistocene uplift of the Qilian Shan (Tapponnier et al., 1982, 2001). By contrast, models emphasizing asthenosphere detachment predicted a synchronous Late

Miocene uplift across the plateau (England and Houseman, 1988; Harrison et al., 1992; Molnar et al., 1993).

Progress has been made regarding the timing of the northeastern Tibetan Plateau, but direct evidence restoring paleoaltimetry of this part of the plateau is scarce. This is mainly because commonly used stable isotope-based paleoaltimetry proxies suffer from the water recycling issue in this region, which prevents a straightforward application of the calibration equation (Tian et al., 2007; Bershaw et al., 2012; Li and Garzione, 2017). In order to get a clear understanding of the uplift history of the northeastern Tibetan Plateau, other approaches are needed (Deng and Ding, 2015; Jiang et al., 2015; Li and Garzione, 2017; Wang and Liu, 2021).

Bacterial-branched glycerol dialkyl glycerol tetraethers (brGDGTs) hold great promise in deriving paleoelevation in this part of the Tibetan Plateau because it links elevation with mean annual air temperature (MAAT) (Sinninghe Damsté et al., 2008; Peterse et al., 2009; Liu et al., 2013; Bai et al., 2018; Guo et al., 2018; Zhuang et al., 2019; Wang and Liu, 2021). However, there is no MAAT–brGDGTs transfer function available for the Qilian Shan area, the major highland of the northeastern Tibetan Plateau, hindering quantitative reconstruction of the elevation history. Here, we report the first MAAT–brGDGTs transfer equation using soils from an elevation transect of the eastern Qilian Shan.

MATERIALS AND METHODS

Study Site and Sampling

The eastern part of the Qilian Shan is located in the confluence zone of the high cold region of the Tibetan Plateau, the northwest inland arid region and the eastern monsoon region (Li and Feng, 1988). The characteristics of the vertical climate zone are obvious. In this region, precipitation increases with altitude, and temperature decreases with altitude (Yang and Liu, 2012; Wu et al., 2014; Wang et al., 2017). Precipitation is mainly concentrated in summer. According to previous studies (Wu et al., 2014; Wang et al., 2017; Ma, 2020), the basins below 2,200 m above the sea level have typical climatic characteristics of the semiarid steppe, with the annual average temperature of 7.4–9.6°C and the annual average precipitation of 230–260 mm; in the foothills, at an altitude of 2,400–2,600 m, the annual average temperature is between 3.4 and 5°C, and the annual average precipitation is between 250 and 500 mm; the region with an altitude of 2,800–3,000 m has a semi-humid forest-steppe climate, with the annual average temperature of 0–3°C and the annual average precipitation of 500–600 mm. The subalpine and alpine regions above 3,000 m above the sea level have an alpine climate, with the annual average temperature below -5°C and the annual average precipitation of ~800 mm. Due to the complex topography and geomorphology, the vegetation also shows the characteristics of diversity and vertical variation (Wu et al., 2014; Ma, 2020).

A total of nine soil samples ranging from 2,055 to 3,300 m of the eastern Qilian Shan were collected. The study area has a small horizontal span and a large elevation gradient, so it is a good area to study the relationship between brGDGTs and altitude. The collected area is covered by natural vegetation. To make sure fresh soils were collected, we removed the top 10 cm soils before taking the samples. Immediately after the samples were collected, we packed them in sealed bags.

A total of three instruments were set up to monitor temperature and precipitation variations from 2,060 to 3,070 m over the year 2005–2020, and one instrument was set up at 3,600 m over the year 2016–2020 (**Figure 1**). The temperature decreases and precipitation increases while moving up to higher elevation in the Qilian Shan (**Supplementary Table S1**). We obtained the temperature and precipitation data from each sampling location based on interpolation of data from these. The results showed that as the altitude rises from 2,055 to 3,300 m, the MAAT drops from 7.7 to −0.8°C, and the mean annual precipitation (MAP) rises from 241.4 to 549.8 mm.

GDGTs Pretreatment and Analysis

Plant roots and gravels were picked out from the nine samples, and then we screened them using a 60-mesh sieve. Freeze-dried samples weighing 10–15 g were ultrasonically agitated in dichloromethane:methanol (9:1, v/v) four times, and the total lipid extract was concentrated under N_2 gas and then saponified for 12 h with 6% KOH/methanol solution. The total lipid extract was separated over a silica gel using hexane, dichloromethane, and methanol as eluents to isolate the apolar and polar fractions (containing GDGTs). The polar fractions of these samples were redissolved and filtered through a 0.22 μm PTFE filter prior to analysis.

The determination of GDGTs compounds was carried out at the Key Laboratory of Western China's Environmental Systems (Ministry of Education), Lanzhou University. The GDGTs analyses were performed using an Agilent 1290 series ultra-performance liquid chromatography–atmospheric pressure chemical ionization–6465B triple quadrupole mass spectrometry (UPLC-APCI-MS) system. When the flow rate was 0.2 ml/min, an aliquot of 15 μL was injected and separated on three Hypersil GOLD Silica columns in sequence (each 100 mm × 2.1 mm, 1.9 μm, Thermo Fisher Scientific; United States), maintained at 40°C. GDGTs were eluted isocratically with 84% A and 16% B for first 5 min, where A = n-hexane and B = EtOA, followed by a linear gradient change to 82% A and 18% B from 5 to 65 min and then changed to 100% B for 15 min, and then back to 84% A and 16% B to equilibrate the pressure. Analyses were performed using the selective ion monitoring (SIM) mode to track *m*/*z* 1302, 1300, 1298, 1296, 1292, 1050, 1048, 1046, 1036, 1034, 1032, 1022, 1020, and 1018, and the GDGTs compounds were identified as GDGT-0, GDGT-1, GDGT-2, GDGT-3, Cren (Cren'), IIIa (IIIa'), IIIb (IIIb'), IIIc (IIIc'), IIa (IIa'), IIb (IIb'), IIc (IIc'), Ia, Ib, and Ic.

We measured the pH values of soils according to the method described by Weijers et al. (2007a). First, samples were ground to powder and then mixed with ultrapure water, using the ratio of soil to water of 1:2.5 mg/L. Then, samples were centrifuged for 5 min at 3,000 revolutions, followed by measuring the pH value of

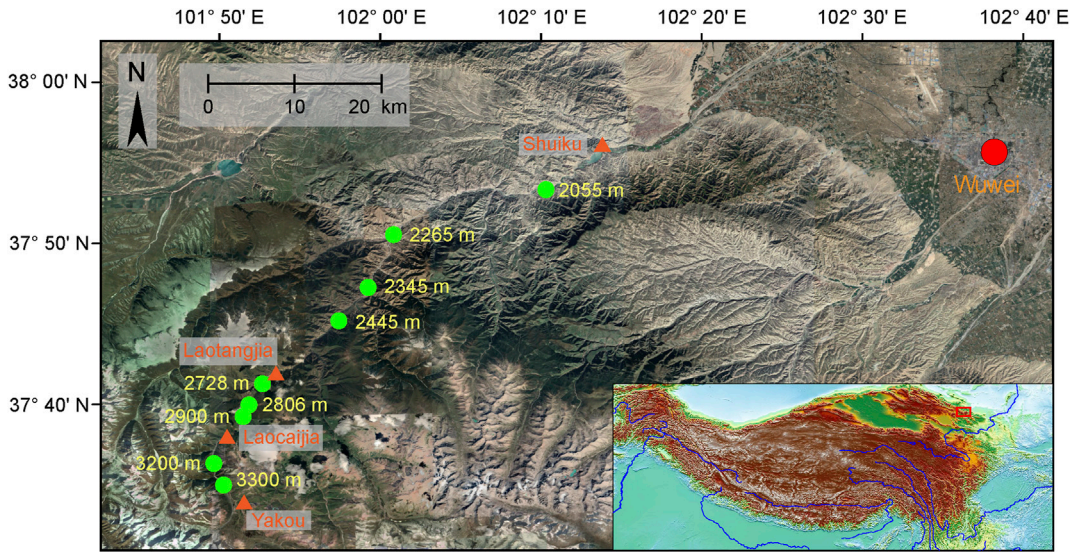

FIGURE 1 | Topographic map of the Qilian Shan and sampling sites (green dots). The red triangles indicate the locations of the four meteorological meters. Revised from Gao et al. (2021). The base map is from Google Image.

the upper supernatant using a pH meter. Each sample was measured three times, and the average values were reported.

BrGDGTs-Based Temperature Indices

Using brGDGTs to derive temperature relies on the following indices: methylation of branched tetraethers (MBT), $MBT'_{5ME\ (5\text{-methyl})}$, $MBT'_{6ME\ (6\text{-methyl})}$, Index 1, and $MBT_{5/6}$ (Weijers et al., 2007b; De Jonge et al., 2014a; Ding et al., 2015), where

$$MBT = ([Ia] + [Ib] + [Ic])/([Ia] + [Ib] + [Ic] + [IIa] + [IIa'] + [IIb] + [IIb'] + [IIc] + [IIc'] + [IIIa] + [IIIa'] + [IIIb] + [IIIb'] + [IIIc] + [IIIc']); \quad (1)$$

$$MBT_{5/6} = ([Ia] + [Ib] + [Ic] + [IIa'])/([Ia] + [Ib] + [Ic] + [IIc] + [IIb] + [IIa] + [IIIa] + [IIIa']); \quad (2)$$

$$MBT'_{5ME} = ([Ia] + [Ib] + [Ic])/([Ia] + [Ib] + [Ic] + [IIa] + [IIb] + [IIc] + [IIIa]); \quad (3)$$

$$MBT'_{6ME} = ([Ia] + [Ib] + [Ic])/([Ia] + [Ib] + [Ic] + [IIa'] + [IIb'] + [IIc'] + [IIIa'] + [IIIb'] + [IIIc']); \quad (4)$$

$$\text{Index 1} = 10^{\log([Ia] + [Ib] + [Ic] + [IIa'] + [IIIa'])/([Ic] + [IIa] + [IIc] + [IIIa] + [IIIa'])}. \quad (5)$$

In the aforementioned formulas, the Roman numbers and letters with the sign [] represent the relative abundance of a single brGDGT compound.

The pH-based brGDGTs substitution metrics used in this article include cyclization of branched tetraethers (CBTs) (Weijers et al., 2007b)

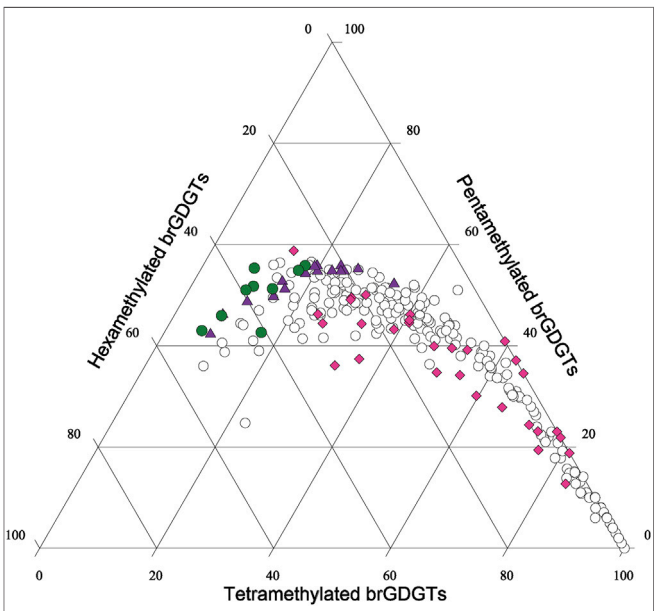

FIGURE 2 | Relative abundance of tetramethylene, pentamethylene, and hexamethylene in branched glycerol dialkyl glycerol tetraethers (brGDGTs). The green circles correspond to soils used in this article. The purple triangles correspond to soils from the northeastern Tibetan Plateau reported by Wang and Liu, 2021, and the pink solid diamonds correspond to soils from the northeastern Tibetan Plateau reported by Chen et al. (2019). The solid white circles correspond to global soils reported by De Jonge et al. (2014a).

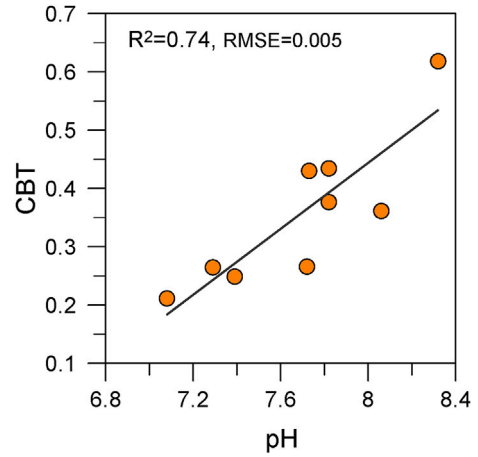

FIGURE 3 | Correlation between CBT and pH.

$$CBT = -^{10}\log\left([Ib] + [IIb] + \left[IIb^{'}\right]\right)/\left([Ia] + [IIa] + \left[IIa^{'}\right]\right). \quad (6)$$

To convert brGDGTs to temperature, four ways have been proposed:

$$MAAT = -8.57 + 31.45 \times MBT^{'}_{5ME} \quad (De\ Jonge\ et\ al., 2014a); \quad (7)$$

$$MAAT = 5.05 + 14.86 \times Index\ 1 \quad (De\ Jonge\ et\ al., 2014a); \quad (8)$$

$$MAAT = -20.14 + 39.51 \times MBT_{5/6} \quad (Ding\ et\ al., 2015); \quad (9)$$

$$MAAT = (MBT - 0.122 - 0.187 \times CBT)/0.02 \quad (Weijers\ et\ al., 2007b). \quad (10)$$

Equations 7, **8** are based on soils of a widely distributed area, **Eq. 9** is based on Tibetan Plateau soils, and **Eq. 10** is also based on global soils.

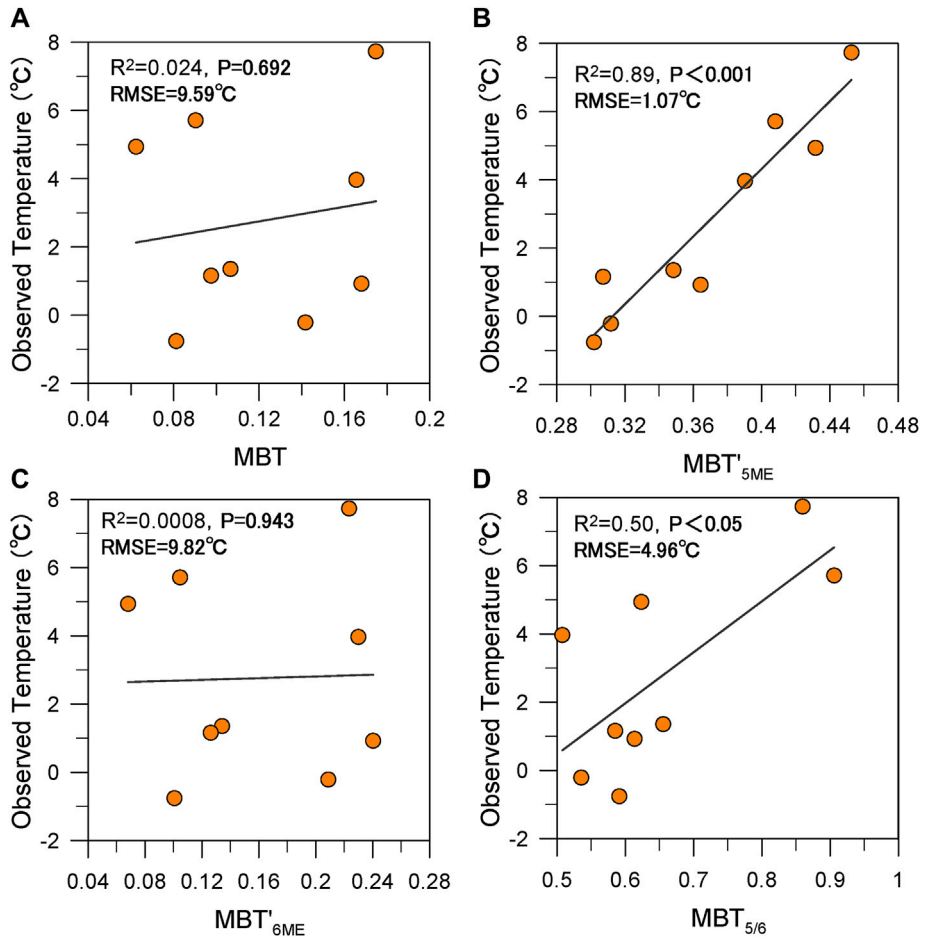

FIGURE 4 | Correlation diagrams between brGDGTs index and temperature. **(A)** Correlation between MBT'_{5ME} and temperature; **(B)** correlation between MBT'_{6ME} and temperature; **(C)** correlation between $MBT_{5/6}$ and temperature; and **(D)** correlation between MBT and temperature.

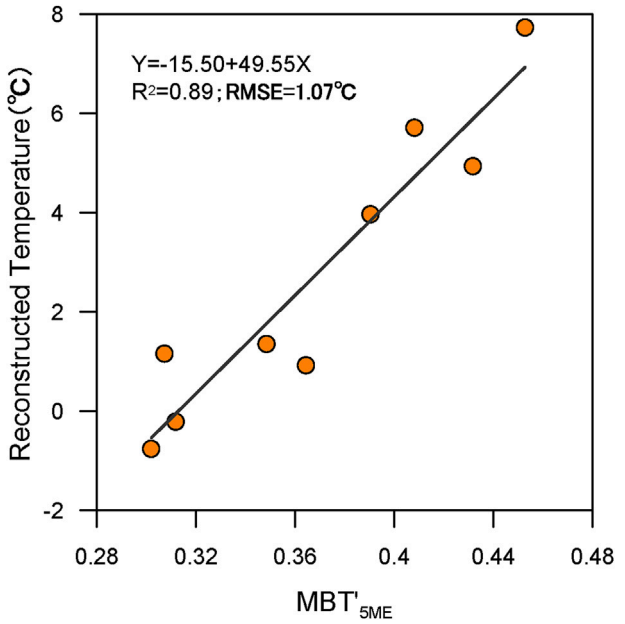

FIGURE 5 | Reconstructed Qilian Shan soil temperatures based on MBT'_{5ME}.

RESULTS

BrGDGTs were detected in all samples (**Supplementary Table S2**). **Figure 2** shows that the relative abundance of pentamethylation, hexamethylation, and tetramethylation is the highest (50.2 ± 7.6%) with the former and the lowest (12.1 ± 5.9%) with the latter. The relative abundance of IIIc and IIIc' detected in each sample is low. In comparison with previous results (De Jonge et al., 2014b; Chen et al., 2019; Wang and Liu, 2021), the Qilian Shan surface soils are located at the end of low tetramethylation.

Figure 3 shows a significant positive correlation between pH and CBT (R^2 = 0.74, RMSE = 0.005). **Figure 4** shows the correlation between the temperature and MBT'_{5ME}, $MBT_{5/6}$, MBT, or MBT'_{6ME}, with the strongest correlation with MBT'_{5ME} and lack of correlation with the latter two. We thus estimate the MAAT based on the equation between MBT'_{5ME} and temperature (**Figure 5**). **Figure 6** shows the correlation between observed and estimated MAAT based on **Equations 7–10**. It is clear that the results based on **Eq. 7** and our own equation have high correlation, but the results based on our own calibration have smaller intercept than that of **Eq. 7**.

Figure 7 shows the correlation between the estimated MAAT based on our own calibration equation and elevation. A

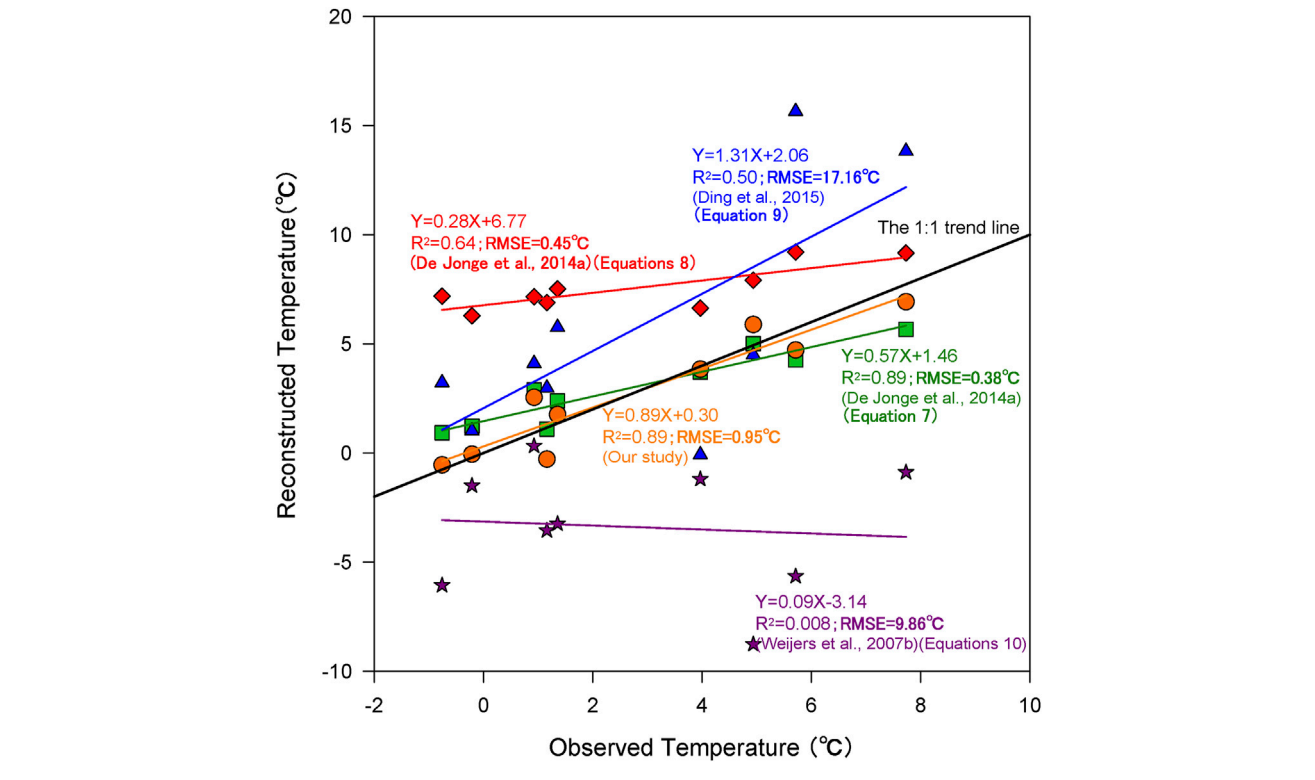

FIGURE 6 | Correlation between reconstructed temperature and observed temperature.

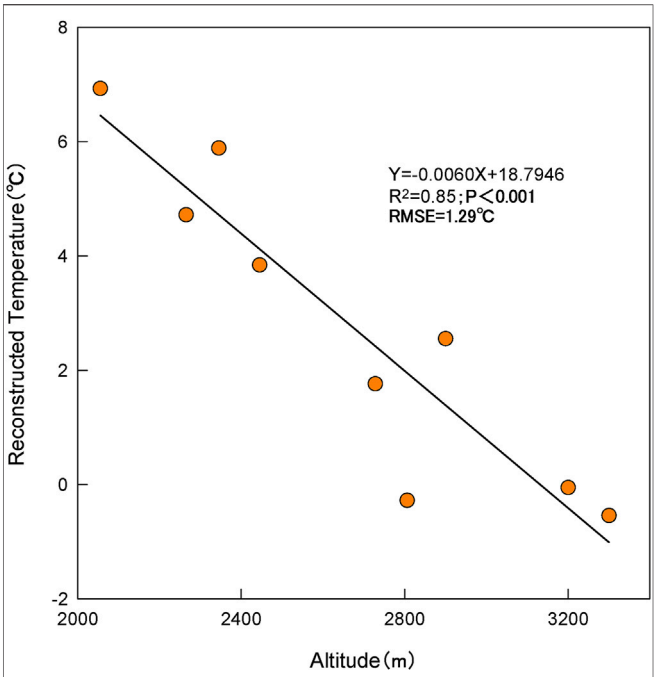

FIGURE 7 | Correlation between brGDGTs-derived temperature estimation and altitude of the Qilian Shan samples.

significant linear negative correlation is observed between them (R^2 = 0.85, p < 0.001, RMSE = 1.29°C).

DISCUSSION

Weijers et al. (2007b) found a negative correlation between CBT and pH based on soils from 90 globally distributed locations, and this pattern has been confirmed by many groups using soils from Lake Qinghai of the northeastern Tibetan Plateau and global soils (Peterse et al., 2012; Wang et al., 2012). Similarly, our work found a significant correlation between CBT and pH (R^2 = 0.74, RMSE = 0.005). But unlike the previous results of others, there is a positive correlation between CBT and pH rather than a negative correlation (**Figure 3**). After repeated experiments, we found that the results of many experiments were highly consistent. Through the study of modern Chinese soils, some scholars have found that when pH > 7.5 and MAP <600 mm, there is a positive correlation between CBT and pH (Xie et al., 2012). Our results fully support this claim because the pH values of our samples are greater than 7.5, and the precipitation varies from 241.4 to 549.8 mm. Our work reveals that the traditional CBT-derived pH correction equation may not be suitable for alkaline soils in arid climate, and it is important to evaluate these two factors before applying established pH calibration equations based on CBT.

We found a significant correlation between MBT'_{5ME} index excluding 6-methyl brGDGTs and MAAT (R^2 = 0.89, p < 0.001, RMSE = 1.07°C) for the Qilian Shan transect samples (**Figure 4**). This pattern is consistent with the results based on a much broader soil database by De Jonge et al., 2014a, De Jonge et al., 2014b (n = 222, R^2 = 0.66, RMSE = 4.8°C). Therefore, this proxy is a more promising one for paleotemperature and paleoaltimetry reconstruction than MBT and MBT′ in the study area.

The analysis of the environmental factors of the relative distribution of brGDGTs isomers shows that the change in MBT seems to be determined by both pH and MAAT, whereas CBT is mainly determined by pH (Weijers et al., 2006; Weijers et al., 2007b). Therefore, temperature can be reconstructed by combining MBT and CBT (Weijers et al., 2007a; Weijers et al., 2007b). However, the correlation between reconstructed temperature and combined using MBT and CBT still exhibits some problems in some areas. For example, in Siberia, Serbia, and East Africa, temperature estimates based on MBT/CBT for MIS 5 are higher than those for MIS 2, and this has been proposed to be caused by the growth depth effect of GDGTs (Zech et al., 2012). When using the MBT′/CBT correction formula based on global soil samples in arid and semiarid areas, workers found that the calculated temperatures are lower than the measured values, which may be because rainfall is the main controlling factor affecting the climatic environment in arid and semiarid areas (Peterse et al., 2011a; Wang et al., 2013). Previous studies have elaborated the underlying reason why MBT and MBT′ have weaker correlation with temperature, and the mechanism is associated with 6-methyl brGDGTs (Li et al., 2017). It has been suggested that the soil pH indirectly affects the correlation between MBT or MBT′ and MAAT by affecting the content of 6-methyl brGDGTs in soils (Yang et al., 2015; Chen et al., 2021). Therefore, both pH and temperature control MBT or MBT′. In addition to pH, some propose that MBT and MBT′ indices in arid–semiarid areas are also affected by soil moisture (Loomis et al., 2011; Menges et al., 2014; Yang et al., 2014; Dang et al., 2016), further weakening its correlation with temperature (Naafs et al., 2017). The reconstructed MAAT based on MBT'_{5ME} has the best correlation with observed MAAT (**Figure 6**), providing further confirmation of the usefulness of MBT'_{5ME} in paleoelevation and paleotemperature reconstructions.

Figure 6 shows that the calibration between MBT'_{5ME} and temperature based on global soils also has high correlation with the result based on Qilian Shan soils. However, we argue that the local calibration equation is better than that based on global soils. First, the slope between estimated and observed MAAT is closer to 1 using the local calibration equation. Second, the local equation has smaller intercept than the one based on global soils. The better match with the observed MAAT using the Qilian Shan soils may be because the Qilian Shan soils have higher 6-methyl brGDGTs. Some scholars pointed out that the 6-methyl brGDGTs in the surface soils of the Tibetan Plateau account for about 53% of brGDGTs, which is significantly higher than the global average of 24% (Ding et al., 2015). In our work, the 6-methyl brGDGTs are 37.7 ± 13.1%, clearly different from that of global soils.

Some studies on soil datasets in China have pointed out that in relatively cold areas (observed MAAT <6°C), the temperature

reconstructed based on MATmr may greatly overestimate observation temperature (Wang et al., 2020), such as the Laji Mountains in the northeastern Tibetan Plateau (Wang and Liu, 2021). This is consistent with our research results. Also, our work found that the deviation between MATmr and the observed temperature increases with altitude (**Supplementary Figure S1**). The reason for this deviation may be because that the microorganisms that produce GDGTs are more suitable for growing in warm and humid conditions, so the estimated temperature may be more biased toward the growing season temperature of GDGTs (Peterse et al., 2011b; Peterse et al., 2014; Zeng and Yang, 2019). Another possibility is that the microbes living in the soils may reflect relatively high soil temperatures rather than relatively cold atmospheric temperatures (Gao et al., 2012; Wang et al., 2016). There is a great difference between soil temperature and atmospheric temperature in cold areas. These results suggest that there are limitations when using MATmr to estimate paleotemperature and paleoaltitude in relatively cold areas (observed MAAT <8°C). It may underestimate the height of uplift.

Many studies have shown that the calibration equation between brGDGTs index and temperature varies in different regions and soil types (Sinninghe Damsté et al., 2008; Bendle et al., 2010; Yang et al., 2015). Therefore, it is inappropriate to use the conversion equation in other areas to infer paleotemperature and paleoelevation variation in an area with different temperature and precipitation ranges and seasonality and vegetation (Sinninghe Damsté et al., 2008; Bendle et al., 2010). We recommend using MBT'_{5ME} to reflect the temperature change in the Qilian Shan area and establish the conversion equation between MBT'_{5ME} and MAAT as follows (**Figure 5**):

$$MAAT = -15.50 + 49.55 \times MBT'_{5ME} \left(R^2 = 0.89, p < 0.001, RMSE = 1.07^{\circ}C\right); \quad (11)$$

We further establish the calibration between MBT'_{5ME}-derived MAAT and altitude as follows:

$$MAAT = 18.7946 - 0.0060 \times altitude \left(R^2 = 0.85, p < 0.001, RMSE = 1.29^{\circ}C\right); \quad (12)$$

The best applicable condition for the correction equation we established is the alkaline soil in the arid and semiarid regions of the northeastern Tibetan Plateau.

We note that the MAAT reconstructed using **Equations 11**, **12** showed an obvious linear negative correlation with altitude, which decreased from 6.93°C at 2,055 m to −0.54°C at 3,300 m (**Figure 7**). The lapse rate associated with the reconstructed temperature based on our equations is −0.60°C/100 m, similar to that based on observed temperatures from the meteorological meters that we set (−0.67°C/100 m). This lapse rate is also similar to reported lapse rates from the northern slope of the Qilian Shan (−0.58°C/100 m) (Zhang et al., 2001) and the neighboring Laji Mountain (−0.65°C/100 m) (Wang and Liu, 2021). However, one study reported a lower lapse rate from the south slope of Lenglongling in the Qilian Shan (−0.51°C /100 m) from higher elevations (elevation 3,200–4,300 m) and higher precipitation ranges (Wang et al., 2009). We speculate that this difference is due to the obvious effect of air humidity on the temperature lapse rate. Some studies have shown that the increase of air humidity will lead to the decrease of the temperature lapse rate (Guo et al., 2016). In addition, higher elevations have different vegetation conditions which may also affect temperature reconstruction due to potential 6-methyl brGDGTs content variations (Liang et al., 2019; Lu et al., 2019).

CONCLUSION

To test the accuracy and applicability of brGDGTs as a paleo-altimeter in the Qilian Shan area, we analyzed the brGDGTs distribution from soil in Lenglongling in the east of Qilian Shan with elevation ranges of 2,055–3,300 m. We demonstrate that MBT'_{5ME} has a good correlation with temperature and altitude in this area and establish a conversion equation between MBT'_{5ME} and MAAT (elevation). This transfer equation is superior to the ones based on global soils, and we recommend using our equations to reconstruct elevation and temperature history in the Qilian Shan and areas with similar climate.

DATA AVAILABILITY STATEMENT

The original contributions presented in the study are included in the article/**Supplementary Material**; further inquiries can be directed to the corresponding authors.

AUTHOR CONTRIBUTIONS

The idea for this article was provided by the corresponding authors JN, AZ, and BP, who also guided and modified the work of this manuscript. HW wrote the manuscript and drew the diagrams. PG conducted sample collection on site. RY carried out the experimental work. BC provided the weather station data. JP and LC provided many suggestions for this article.

FUNDING

This work was financially supported by the Second Tibetan Plateau Scientific Expedition (grant 2019QZKK0704) and National Natural Science Foundation of China (grant 41888101).

SUPPLEMENTARY MATERIAL

The Supplementary Material for this article can be found online at: https://www.frontiersin.org/articles/10.3389/feart.2022.844026/full#supplementary-material

REFERENCES

And, L. J., Zhaodon, F., and Lingyu, T. (1988). Late Quaternary Monsoon Patterns on the Loess Plateau of China. *Earth Surf. Process. Landforms* 13 (12), 125–135. doi:10.1002/esp.3290130204

Bai, Y., Chen, C., Xu, Q., and Fang, X. (2018). Paleoaltimetry Potentiality of Branched GDGTs from Southern Tibet. *Geochem. Geophys. Geosyst.* 19 (2), 551–564. doi:10.1002/2017gc007122

Bendle, J. A., Weijers, J. W. H., Maslin, M. A., Sinninghe Damsté, J. S., Schouten, S., Hopmans, E. C., et al. (2010). Major Changes in Glacial and Holocene Terrestrial Temperatures and Sources of Organic Carbon Recorded in the Amazon Fan by Tetraether Lipids. *Geochem. Geophys. Geosyst.* 11 (12), Q12007. doi:10.1029/2010gc003308

Bershaw, J., Penny, S. M., and Garzione, C. N. (2012). Stable Isotopes of Modern Water across the Himalaya and Eastern Tibetan Plateau: Implications for Estimates of Paleoelevation and Paleoclimate. *J. Geophys. Res.* 117 (D2), D02110. doi:10.1029/2011jd016132

Chen, C., Bai, Y., Fang, X., Guo, H., Meng, Q., Zhang, W., et al. (2019). A Late Miocene Terrestrial Temperature History for the Northeastern Tibetan Plateau's Period of Tectonic Expansion. *Geophys. Res. Lett.* 46 (14), 8375–8386. doi:10.1029/2019gl082805

Chen, C., Bai, Y., Fang, X., Zhuang, G., Khodzhiev, A., Bai, X., et al. (2021). Evaluating the Potential of Soil Bacterial Tetraether Proxies in Westerlies Dominating Western Pamirs, Tajikistan and Implications for Paleoenvironmental Reconstructions. *Chem. Geology.* 559, 119908. doi:10.1016/j.chemgeo.2020.119908

Chung, S.-L., Chu, M.-F., Zhang, Y., Xie, Y., Lo, C.-H., Lee, T.-Y., et al. (2005). Tibetan Tectonic Evolution Inferred from Spatial and Temporal Variations in post-collisional Magmatism. *Earth-Science Rev.* 68 (3-4), 173–196. doi:10.1016/j.earscirev.2004.05.001

Dang, X., Yang, H., Naafs, B. D. A., Pancost, R. D., and Xie, S. (2016). Evidence of Moisture Control on the Methylation of Branched Glycerol Dialkyl Glycerol Tetraethers in Semi-arid and Arid Soils. *Geochimica et Cosmochimica Acta* 189, 24–36. doi:10.1016/j.gca.2016.06.004

De Jonge, C., Hopmans, E. C., Zell, C. I., Kim, J.-H., Schouten, S., and Sinninghe Damsté, J. S. (2014a). Occurrence and Abundance of 6-methyl Branched Glycerol Dialkyl Glycerol Tetraethers in Soils: Implications for Palaeoclimate Reconstruction. *Geochimica et Cosmochimica Acta* 141, 97–112. doi:10.1016/j.gca.2014.06.013

De Jonge, C., Stadnitskaia, A., Hopmans, E. C., Cherkashov, G., Fedotov, A., and Sinninghe Damsté, J. S. (2014b). *In Situ* produced Branched Glycerol Dialkyl Glycerol Tetraethers in Suspended Particulate Matter from the Yenisei River, Eastern Siberia. *Geochimica et Cosmochimica Acta* 125, 476–491. doi:10.1016/j.gca.2013.10.031

Deng, T., and Ding, L. (2015). Paleoaltimetry Reconstructions of the Tibetan Plateau: Progress and Contradictions. *Natl. Sci. Rev.* 2 (4), 417–437. doi:10.1093/nsr/nwv062

Ding, S., Xu, Y., Wang, Y., He, Y., Hou, J., Chen, L., et al. (2015). Distribution of Branched Glycerol Dialkyl Glycerol Tetraethers in Surface Soils of the Qinghai-Tibetan Plateau: Implications of brGDGTs-Based Proxies in Cold and Dry Regions. *Biogeosciences* 12 (11), 3141–3151. doi:10.5194/bg-12-3141-2015

England, P. C., and Houseman, G. A. (1988). The Mechanics of the Tibetan Plateau. *Phil. Trans. R. Soc. Lond. A.* 326 (1589), 301–320. doi:10.1098/rsta.1988.0089

Fielding, E. J. (1996). Tibet Uplift and Erosion. *Tectonophysics* 260, 55–84. doi:10.1016/0040-1951(96)00076-5

Gao, L., Nie, J., Clemens, S., Liu, W., Sun, J., Zech, R., et al. (2012). The Importance of Solar Insolation on the Temperature Variations for the Past 110kyr on the Chinese Loess Plateau. *Palaeogeogr. Palaeoclimatol. Palaeoecol.* 317, 128–133. doi:10.1016/j.palaeo.2011.12.021

Gao, P., Nie, J., Yan, Q., Zhang, X., Liu, Q., Cao, B., et al. (2021). Millennial Resolution Late Miocene Northern China Precipitation Record Spanning Astronomical Analogue Interval to the Future. *Geophys. Res. Lett.* 48 (15), e2021GL093942.

Guo, H. C., Chen, C. H., and Bai, Y. (2018). Paleoenvironmental Evolution of the Xining Basin, NE Tibetan Plateau during Mid-miocene: Revealed by GDGTs. *Quat. Sci.* 38, 97–106. doi:10.11928/j.issn.1001-7410.2018.01.08

Guo, X., Wang, L., and Tian, L. (2016). Spatio-temporal Variability of Vertical Gradients of Major Meteorological Observations Around the Tibetan Plateau. *Int. J. Climatol.* 36 (4), 1901–1916. doi:10.1002/joc.4468

Harrison, T. M., Copeland, P., KiDD, W. S. F., and Yin, A. (1992). Raising Tibet. *Science* 255, 1663–1670. doi:10.1126/science.255.5052.1663

Jiang, G. L., Zhang, K. X., and Xu, Y. D. (2015). Research Progress of Quantitative Paleoelevation Reconstruction of Tibetan Plateau. *Adv. Earth Sci.* 30, 334–345. doi:10.11867/j.issn.1001-8166.2015.03.0334

Kristen Clark, M., and Handy Royden, L. (2000). Topographic Ooze: Building the Eastern Margin of Tibet by Lower Crustal Flow. *Geology* 28 (8), 703–706. doi:10.1130/0091-7613(2000)028<0703:tobtem>2.3.co;2

Li, L., and Garzione, C. N. (2017). Spatial Distribution and Controlling Factors of Stable Isotopes in Meteoric Waters on the Tibetan Plateau: Implications for Paleoelevation Reconstruction. *Earth Planet. Sci. Lett.* 460, 302–314. doi:10.1016/j.epsl.2016.11.046

Li, X. M., Zhu, E. L., Wang, M. D., Liang, J., Wang, Z. F., Liang, E. Y., et al. (2017). Distributions of Glycerol Dialkyl Glycerol Tetraether Lips along an Altitudinal Transect on the Southern Slope of MT.Himalaya and Their Indicating Significance. *Quat. Sci.* 37, 1226–1237. doi:10.11928/j.issn.1001-7410.2017.06.07

Liang, J., Russell, J. M., Xie, H., Lupien, R. L., Si, G., Wang, J., et al. (2019). Vegetation Effects on Temperature Calibrations of Branched Glycerol Dialkyl Glycerol Tetraether (brGDGTs) in Soils. *Org. Geochem.* 127, 1–11. doi:10.1016/j.orggeochem.2018.10.010

Liu, W., Wang, H., Zhang, C. L., Liu, Z., and He, Y. (2013). Distribution of Glycerol Dialkyl Glycerol Tetraether Lipids along an Altitudinal Transect on Mt. Xiangpi, NE Qinghai-Tibetan Plateau, China. *Org. Geochem.* 57, 76–83. doi:10.1016/j.orggeochem.2013.01.011

Liu, X., Xu, Q., and Ding, L. (2016). Differential Surface Uplift: Cenozoic Paleoelevation History of the Tibetan Plateau. *Sci. China Earth Sci.* 59 (11), 2105–2120. doi:10.1007/s11430-015-5486-y

Liu, X., and Yin, Z.-Y. (2002). Sensitivity of East Asian Monsoon Climate to the Uplift of the Tibetan Plateau. *Palaeogeogr. Palaeoclimatol. Palaeoecol.* 183, 223–245. doi:10.1016/S0031-0182(01)00488-6

Loomis, S. E., Russell, J. M., and Sinninghe Damsté, J. S. (2011). Distributions of Branched GDGTs in Soils and lake Sediments from Western Uganda: Implications for a Lacustrine Paleothermometer. *Org. Geochem.* 42 (7), 739–751. doi:10.1016/j.orggeochem.2011.06.004

Lu, C. X., Yu, G., and Xie, G. D. (2005). Tibetan Plateau Serves as a Water Tower. in *International Geoscience and Remote Sensing Symposium*. Seoul, Korea: Ieee.

Lu, H., Liu, W., Yang, H., Wang, H., Liu, Z., Leng, Q., et al. (2019). 800-kyr Land Temperature Variations Modulated by Vegetation Changes on Chinese Loess Plateau. *Nat. Commun.* 10 (1), 1–10. doi:10.1038/s41467-019-09978-1

Ma, Z. H. (2020). "Layered Landforms and Drainage Evolution in the Eastern Qilian Mountains since Late Miocene," (Lanzhou: Lanzhou University). phd thesis.

Menges, J., Huguet, C., Alcañiz, J. M., Fietz, S., Sachse, D., and Rosell-Melé, A. (2014). Influence of Water Availability in the Distributions of Branched Glycerol Dialkyl Glycerol Tetraether in Soils of the Iberian Peninsula. *Biogeosciences* 11 (10), 2571–2581. doi:10.5194/bg-11-2571-2014

Molnar, P., Boos, W. R., and Battisti, D. S. (2010). Orographic Controls on Climate and Paleoclimate of Asia: Thermal and Mechanical Roles for the Tibetan Plateau. *Annu. Rev. Earth Planet. Sci.* 38 (1), 77–102. doi:10.1146/annurev-earth-040809-152456

Molnar, P., England, P., and Martinod, J. (1993). Mantle Dynamics, Uplift of the Tibetan Plateau, and the Indian Monsoon. *Rev. Geophys.* 31 (4), 357–396. doi:10.1029/93RG02030

Naafs, B. D. A., Gallego-Sala, A. V., Inglis, G. N., and Pancost, R. D. (2017). Refining the Global Branched Glycerol Dialkyl Glycerol Tetraether (brGDGT) Soil Temperature Calibration. *Org. Geochem.* 106, 48–56. doi:10.1016/j.orggeochem.2017.01.009

Peterse, F., Hopmans, E. C., Schouten, S., Mets, A., Rijpstra, W. I. C., and Sinninghe Damsté, J. S. (2011a). Identification and Distribution of Intact Polar Branched Tetraether Lipids in Peat and Soil. *Org. Geochem.* 42 (9), 1007–1015. doi:10.1016/j.orggeochem.2011.07.006

Peterse, F., Martínez-García, A., Zhou, B., Beets, C. J., Prins, M. A., Zheng, H., et al. (2014). Molecular Records of continental Air Temperature and Monsoon

Precipitation Variability in East Asia Spanning the Past 130,000 Years. *Quat. Sci. Rev.* 83, 76–82. doi:10.1016/j.quascirev.2013.11.001

Peterse, F., Prins, M. A., Beets, C. J., Troelstra, S. R., Zheng, H., Gu, Z., et al. (2011b). Decoupled Warming and Monsoon Precipitation in East Asia over the Last Deglaciation. *Earth Planet. Sci. Lett.* 301 (1-2), 256–264. doi:10.1016/j.epsl.2010.11.010

Peterse, F., van der Meer, J., Schouten, S., Weijers, J. W. H., Fierer, N., Jackson, R. B., et al. (2012). Revised Calibration of the MBT-CBT Paleotemperature Proxy Based on Branched Tetraether Membrane Lipids in Surface Soils. *Geochimica et Cosmochimica Acta* 96, 215–229. doi:10.1016/j.gca.2012.08.011

Peterse, F., van Der Meer, M. T. J., Schouten, S., Jia, G., Ossebaar, J., Blokker, J., et al. (2009). Assessment of Soil N-Alkane δD and Branched Tetraether Membrane Lipid Distributions as Tools for Paleoelevation Reconstruction. *Biogeosciences* 6 (12), 2799–2807. doi:10.5194/bg-6-2799-2009

Raymo, M. E., and Ruddiman, W. F. (1992). Tectonic Forcing of Late Cenozoic Climate. *Nature* 359, 117–122. doi:10.1038/359117a0

Royden, L. H., Burchfiel, B. C., and van der Hilst, R. D. (2008). The Geological Evolution of the Tibetan Plateau. *Science* 321, 1054–1058. doi:10.1126/science.1155371

Sinninghe Damsté, J. S., Ossebaar, J., Schouten, S., and Verschuren, D. (2008). Altitudinal Shifts in the Branched Tetraether Lipid Distribution in Soil from Mt. Kilimanjaro (Tanzania): Implications for the MBT/CBT continental Palaeothermometer. *Org. Geochem.* 39 (8), 1072–1076. doi:10.1016/j.orggeochem.2007.11.011

Tapponnier, P., Peltzer, G., Le Dain, A. Y., Armijo, R., and Cobbold, P. (1982). Propagating Extrusion Tectonics in Asia: New Insights from Simple Experiments with Plasticine. *Geol* 10 (12), 611–616. doi:10.1130/0091-7613(1982)10<611:petian>2.0.co;2

Tapponnier, P., Zhiqin, X., Roger, F., Meyer, B., Arnaud, N., Wittlinger, G., et al. (2001). Oblique Stepwise Rise and Growth of the Tibet Plateau. *Science* 294 (5547), 1671–1677. doi:10.1126/science.105978

Tian, L., Yao, T., MacClune, K., White, J. W. C., Schilla, A., Vaughn, B., et al. (2007). Stable Isotopic Variations in West China: A Consideration of Moisture Sources. *J. Geophys. Res.* 112, D10112. doi:10.1029/2006jd007718

Wang, H., An, Z., Lu, H., Zhao, Z., and Liu, W. (2020). Calibrating Bacterial Tetraether Distributions towards *In Situ* Soil Temperature and Application to a Loess-Paleosol Sequence. *Quat. Sci. Rev.* 231, 106172. doi:10.1016/j.quascirev.2020.106172

Wang, H., Liu, W., and Lu, H. (2016). Appraisal of Branched Glycerol Dialkyl Glycerol Tetraether-Based Indices for North China. *Org. Geochem.* 98, 118–130. doi:10.1016/j.orggeochem.2016.05.013

Wang, H., and Liu, W. (2021). Soil Temperature and brGDGTs along an Elevation Gradient on the Northeastern Tibetan Plateau: A Test of Soil brGDGTs as a Proxy for Paleoelevation. *Chem. Geology.* 566, 120079. doi:10.1016/j.chemgeo.2021.120079

Wang, H., Liu, W., Zhang, C. L., Liu, Z., and He, Y. (2013). Branched and Isoprenoid Tetraether (BIT) index Traces Water Content along Two Marsh-Soil Transects Surrounding Lake Qinghai: Implications for Paleo-Humidity Variation. *Org. Geochem.* 59, 75–81. doi:10.1016/j.orggeochem.2013.03.011

Wang, H., Liu, W., Zhang, C. L., Wang, Z., Wang, J., Liu, Z., et al. (2012). Distribution of Glycerol Dialkyl Glycerol Tetraethers in Surface Sediments of Lake Qinghai and Surrounding Soil. *Org. Geochem.* 47, 78–87. doi:10.1016/j.orggeochem.2012.03.008

Wang, J. L., Li, Y. N., Du, M. Y., Wang, Q. X., Tang, Y. H., Xue, X. J., et al. (2009). The Features of Microclimate and Vegetation Distribution on the Southern Lenglonglin, Qilian Mountains. *J. Mountain Sci.* 4, 418–426. doi:10.16089/j.cnki

Wang, J., Wang, C., Duo, R. j., Chen, B. y., and Zhou, Y. b. (2017). Main Vegetation Types and Their Distribution of Qilian Mountain Region in Qinghai Province. *Chin. Qinghai J. Anim. Vet. Sci.* 47, 15–20. 1003-7950(2017)06-0015-06.

Weijers, J. W. H., Schefuss, E., Schouten, S., and Damste´, J. S. S. (2007a). Coupled thermal and Hydrological Evolution of Tropical Africa over the Last Deglaciation. *Science* 315, 1701–1704. doi:10.1126/science.1138131

Weijers, J. W. H., Schouten, S., Hopmans, E. C., Geenevasen, J. A. J., David, O. R. P., Coleman, J. M., et al. (2006). Membrane Lipids of Mesophilic Anaerobic Bacteria Thriving in Peats Have Typical Archaeal Traits. *Environ. Microbiol.* 8 (4), 648–657. doi:10.1111/j.1462-2920.2005.00941.x

Weijers, J. W. H., Schouten, S., van den Donker, J. C., Hopmans, E. C., and Sinninghe Damsté, J. S. (2007b). Environmental Controls on Bacterial Tetraether Membrane Lipid Distribution in Soils. *Geochimica et Cosmochimica Acta* 71 (3), 703–713. doi:10.1016/j.gca.2006.10.003

Wu, Z. L., Jia, W. X., Liu, Y. R., and Zhang, Y. S. (2014). Change of Vegetation Coverage in the Qilian Mountains in Recent 10 years. *Arid Zone Research* 106, 48–56. doi:10.13866/j.azr.2014.01.023

Xie, S., Pancost, R. D., Chen, L., Evershed, R. P., Yang, H., Zhang, K., et al. (2012). Microbial Lipid Records of Highly Alkaline Deposits and Enhanced Aridity Associated with Significant Uplift of the Tibetan Plateau in the Late Miocene. *Geology* 40 (4), 291–294. doi:10.1130/g32570.1

Yang, F., and Liu, L. (2012). Study on Occurrence Pattern and Trend of Drought in East Qinghai Province. *Arid Zone Res.* 29, 284–288. doi:10.13866/j.azr.2012.02.021

Yang, H., Lü, X., Ding, W., Lei, Y., Dang, X., and Xie, S. (2015). The 6-methyl Branched Tetraethers Significantly Affect the Performance of the Methylation index (MBT′) in Soils from an Altitudinal Transect at Mount Shennongjia. *Org. Geochem.* 82, 42–53. doi:10.1016/j.orggeochem.2015.02.003

Yang, H., Xiao, W., Jia, C., and Xie, S. (2014). Paleoaltimetry Proxies Based on Bacterial Branched Tetraether Membrane Lipids in Soils. *Front. Earth Sci.* 9 (1), 13–25. doi:10.1007/s11707-014-0464-5

Yin, A., and Harrison, T. M. (2000). Geologic Evolution of the Himalayan-Tibetan Orogen. *Annu. Rev. Earth Planet. Sci.* 28, 211–280. doi:10.1146/annurev.earth.28.1.211

Zech, R., Gao, L., Tarozo, R., and Huang, Y. (2012). Branched Glycerol Dialkyl Glycerol Tetraethers in Pleistocene Loess-Paleosol Sequences: Three Case Studies. *Org. Geochem.* 53, 38–44. doi:10.1016/j.orggeochem.2012.09.005

Zeng, F., and Yang, H. (2019). Temperature Changes Reconstructed from Branched GDGTs on the central Loess Plateau during the Past 130-5 Ka. *Quat. Int.* 503, 3–9. doi:10.1016/j.quaint.2018.04.045

Zhang, H., Wen, Y. L., Ma, L., Chang, Z. Q., and Wang, J. Y. (2001). The Climate Features and Regionalization of Vertical Climatic Zones in the Northern Slope of Qilian Mountains. *J. Mountain Sci.* 6 (06), 497–502. doi:10.16089/j.cnki.1008-2786.2001.06.003

Zhisheng, A., Kutzbach, J. E., Prell, W. L., and Porter, S. C. (2001). Evolution of Asian Monsoons and Phased Uplift of the Himalaya-Tibetan Plateau since Late Miocene Times. *Nature* 411, 62–66. doi:10.1038/35075035

Zhuang, G., Zhang, Y. G., Hourigan, J., Ritts, B., Hren, M., Hou, M., et al. (2019). Microbial and Geochronologic Constraints on the Neogene Paleotopography of Northern Tibetan Plateau. *Geophys. Res. Lett.* 46 (3), 1312–1319. doi:10.1029/2018gl081505

Conflict of Interest: The authors declare that the research was conducted in the absence of any commercial or financial relationships that could be construed as a potential conflict of interest.